Movement of Polymer Segments by Exciplex Emission of Pyrene and *N,N*-Dimethylaniline at the Polymer–Silica Interface

Yuko Hayashi[1,3] **and Kunihiro Ichimura**[2]

Intermolecular interaction between pyrenyl units linked on the silica surface and *N,N*-dimethylaniline (DMA) units of polymer segments coated on the silica was investigated. Exciplex emission between these units was observed. The spectral shape and the intensity of the exciplex emission depended on the sample preparative conditions. Emission decay curves had no rise components, which showed that preformed ground-state complexes between pyrene and DMA existed and there were various microenvironmental sites around the preformed complexes just after sample preparation. Annealing of the samples made the exciplex emission wavelength shift and its intensity increase, which meant that polymer segments that contacted with the silica surface moved to make the stable conformations during annealing. It was revealed that DMA units of polymer segments are more stable when they face to the polymer–silica interface than when they become part of the polymer bulk. After the samples were kept at room temperature for 1 month, the spectra of all the samples became the same, which showed that the most stable conformations of the polymer segments were at the polymer–silica interface.

KEY WORDS: Exciplex; polymer–silica interface; calix[4]resorcinarene; annealing.

INTRODUCTION

In a previous work [1], we obtained the novel information about interfacial phenomena by observation of exciplex emission from solid–liquid interface because the exciplex emission is generated specifically at an interface. Although there are some reports have studied the solid–solid interface by attenuated total reflection infrared (ATR-IR) [2], enhanced nuclear magnetic resonance (NMR) [3], X-ray photoelectron spectroscopy (XPS) [4], and so on, there are no reports that show exciplex emission at the solid–solid interface between two species that link to different solids, which indicates the molecular interaction between the two solids. This report aims at constructing a system to provide information about interfacial microenvironments between silica and a polymer solid using exciplex emission. The following conditions should be satisfied: (1) The system exhibits intermolecular interactions between a fluorescent probe adsorbed on a silica surface and segments of the polymer to display strong exciplex emission; (2) the fluorescent probe on silica shows no excimer emission because wavelengths of an excimer and an exciplex of a fluorophore usually lie in the same region, which makes the system complicated for fluorescence analysis; and (3) the polymer does not fluoresce to simplify the emission system at an interface. To satisfy these conditions, the combination of pyrene and *N,N*-dimethyaniline (DMA) was adopted.

There have been reports on the fluorescence of pyrene adsorbed on silica gel [5–7], and self-assembled

[1] Chemical Resources Laboratory, Tokyo Institute of Technology, 4259 Nagatsuta, Midori-ku, Yokohama 226-8503, Japan.
[2] Research Institute for Science and Technology, Tokyo University of Science, 2641 Yamazaki, Noda-shi, Chiba 278-8510, Japan.
[3] To whom correspondence should be addressed. e-mail: yhayashi@res.titech.ac.jp

monolayers incorporating pyrene groups [8,9]. They show excimer emission, so they are not suitable for the present study because exciplex emission with DMA will be hidden by the pyrenyl excimer [10–12]. This problem essentially can be overcome by the reduction of surface density of pyrenyl groups. As a procedure for modification of a silica surface with controlled density of pyrenyl residues, calix[4]resorcinarene (CRA) was employed in this work; CRA gives rise to self-assembled monomolecular films quite readily, owing to its strong adsorptivity to a silica surface [13–15]. The synthesis of CRA possessing a single pyrenyl group and three alkyl chains was achieved in the previous work [16]. An occupied area of a CRA substituted with eight carboxymethoxy units in a self-assembled monolayer has been reported to be approximately 2.0 nm^2; the distance between centers of molecules is about 1.6 nm [13–15]. In this way, when a length of alkyl linking a pyrenyl group to the CRA framework is short enough, the fluorescent moieties should be well separated in the monolayer to suppress the excimer formation. Because a CPK model of the molecule indicated that a spacer with more than two methylenes is long and flexible enough to permit pyrenyl groups close to each other to form excimer on a surface even though CRA framework was rigid, CRA with a pyrenylmethyl group was ordered for the purpose.

In this context, fluorescence behavior of a CRA derivative possessing a single pyrene unit adsorbed on a silica surface was investigated. Colloidal silica particles were used in this work for the adsorption of the macrocyclic compound owing to marked enlargement of a surface area of silica, leading to enhancement of emission intensity. A polymethacrylate with DMA side chains was synthesized and was placed in contact with the CRA-modified silica surface to follow exciplex emission.

EXPERIMENTAL

Materials

Octacarboxymethoxylated 1-pyrenylmethyltrimethylcalix[4]resorcinarene (**1**) as shown in Scheme 1 was synthesized by the same matter as the previous work [16]. The mixture of CRAs with 1-pyrenylmethyl, which was synthesized according to reference [17], and methyl groups were synthesized followed by esterification with ethyl bromoacetate. The mixture of octaethyl carboxylate CRA derivative with zero pyrenyl and four methyl groups, with one pyrenyl and three methyl groups, two-two, three-one, and four-zero was produced and it was separated into each fraction by high-performance gas
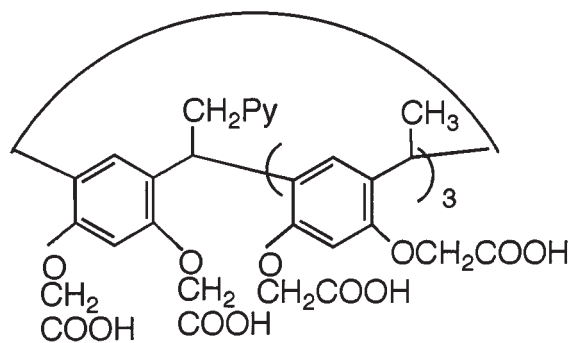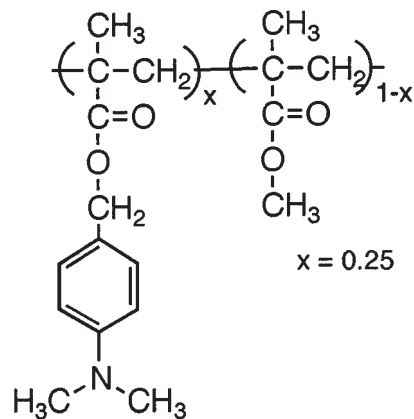

Scheme 1

chromatography (HPLC) (column: SiO$_2$). The CRA derivative possessing one pyrenyl unit was hydrolyzed by KOH to the octacarboxymethoxylated CRA derivative. Relevant data include mp > 300°C (decomp.); ^{1}H-NMR (DMSO-d6); δ (ppm) = 1.46 (d, 9H, J=9.0Hz), 2.24 (s, 2H), 4.38 (s, 16H), 4.4–4.6 (m, 4H), 6.46 (s, 4H), 7.13 (s, 4H), 7.5–8.2 (m, 9H); elemental analysis for C$_{64}$H$_{56}$O$_{24}$4H$_2$O: calculated C, 60.00; H, 5.04%. Found C, 60.27; H, 4.81%.

Poly(4-dimethylaminobenzyl methacrylate-*co*-methyl methacrylate) (**2**) shown in Scheme 2 was also synthesized: Mn = 4.9 × 10^3, Mw = 2.3 × 10^4; dimethylaminobenzyl to methyl ratio = 1:3.0; Tg = 107°C; Elemental analysis for (C$_{13}$H$_{17}$NO$_2$)(C$_5$H$_8$O$_2$)$_{3.0}$: calculated C, 64.71; H, 7.96; N, 2.69%. Found C, 64.47; H, 7.72; N, 2.94%.

Colloidal silica was kindly donated by Nissan Chemical Industry (Tokyo, Japan).

CRA Modification of Colloidal Silica

Colloidal silica of a 73-nm diameter without surface pores was washed ultrasonically in acetone, an aqueous

Scheme 2

NaOH solution, a HNO_3 solution, and finally in water. The colloidal silica was put in a toluene solution of aminopropyldimethylethoxysilane (10 vol%), and the suspension was refluxed for 1 hr, followed by centrifugal separation and ultrasonic washing in toluene. The particles were suspended in toluene again, separated, and dried. The density of the amino group on the silica particles was estimated to be 1.7 groups/nm^2 by the following elemental analysis data on the assumption that a particle is a sphere with a density of 2.3 g/cm^3.

Elemental analysis for the modified colloidal silica was as follows: found C, 0.62; H, 0.48; N, 0.14%.

The aminated colloidal silica was put in a tetrahydrofuran (THF) solution of **1** (1×10^{-4} mol/L) and stirred for 30 min at room temperature. After the colloidal silica was stirred, it was isolated by centrifugal separation. The yellow color of the solution became pale, whereas the modified colloidal silica turned from white to yellowish brown in color, suggesting the adsorption of **1** on the colloidal silica. The colloidal silica was washed in pure acetone ultrasonically, precipitated by centrifugal separation, and dried. The density of pyrenyl group on the silica was calculated as 0.22 groups/nm^2 by the following elemental analysis data. The reacted colloidal silica is abbreviated as Py-CoSi. Elemental analysis for Py-CoSi was as follows: found C, 1.49; H, 0.56; N, 0.13%.

Sample Preparation for the Interfacial Studies

Py-CoSi (100 mg) was placed in 0.5-mL THF or chloroform containing 20 mg of **2**, the suspension was shaken ultrasonically for 30 min, followed by evaporation of the solvent. Annealing samples were achieved by heating.

Measurements

The surface-modified colloidal silica samples covered with a polymer layer were placed in a 0.5-mm-thick quartz cell, and their emission spectra were taken on a JASCO PF-777 (Tokyo, Japan) with the use of the attachment for film. The excitation wavelength for emission spectra was 349 nm for the first peak of $S_0 \rightarrow S_2$ of the pyrenyl chromophore. A DMA unit has no absorption band at this wavelength. All spectra were corrected with that of unreacted colloidal silica as a reference.

Fluorescent lifetime was measured by a single photon counting system with an excitation source of mode-locked Nd: YAG laser and dye laser (rhodamine B), the half-width of which was 0.20 ns operating at 400 kHz.

RESULTS AND DISCUSSION

Effect of Preparative Conditions on Pyrene Fluorescence

For the solvent of a polymer solution, chloroform or THF was adopted. Although they are both good solvents for polymethacrylate, their solvation strengths are different. The solvation to polymethacrylate of THF is strong enough to destroy the adsorption of the polymer on a silica surface, which is caused by the interaction between carbonyl of polymer and silanol of silica surface, whereas polymethacrylate keeps adsorbing on the silica surface in chloroform. This was certified by unpublished results. When a silica plate was immersed in a methacrylate polymer chloroform solution and removed from the solution, the polymer adsorbed on the plate. After the silica plate on which adsorbed polymer was immersed in pure chloroform and removed again, the polymer still adsorbed on the plate. However, when the plate was immersed in pure THF, the polymer dispersed into THF and did not adsorb on the plate when it was removed from the solution.

Two samples of Py-CoSi covered with **2** were prepared with chloroform solution of **2**. The solvent of sample (a) was evaporated under atmosphere at room temperature for a few days and was vacuumed to be removed completely. Sample (b) was not dried under vacuum and solvent can remain in the sample. For comparison, a sample of the Py-CoSi covered without **2** but with a PMMA layer was also prepared from a chloroform solution of poly(methyl methacrylate) (PMMA). Conversely, two samples were also prepared from THF solution of **2**. The solvent of sample (c) was slowly evaporated by the same manner as for sample (a). Sample (d) was evaporated fast under vacuum from the start of the analysis. The solvent evaporating speed influences the microenvironment at the interface when the solvent was THF, which solvates **2** strongly. The prepared samples are summarized in Table I.

Fluorescence spectra of samples (a), (b), and PMMA-coated sample normalized at 379 nm are shown in Fig. 1. The samples were excited at 349 nm so that the emission came specifically from the pyrene S_0 to S_2 region. Although the PMMA sample displayed only the monomer emission, broad emission at a long-wavelength region was observed for the other samples covered with **2**. It follows that the emission bands at a longer wavelength region did not arise from the excimer, but rather from exciplex between the surface pyrene and DMA tethered to polymer chains. This was the first observation of exciplex emission at an interface between two kinds of solids. Sample (b) without vacuum treatment showed

Table I. Preparation of Samples

Sample	Solvent of a polymer solution	Evaporation of solvent	Vaccum after evaporation
Py-CoSi–**2** (a)	Chloroform	Under atmosphere	Yes
Py-CoSi–**2** (b)	Chloroform	Under atmosphere	No
Py-CoSi–**2** (c)	Tetrahydrofuran	Under atmosphere	Yes
Py-CoSi–**2** (d)	Tetrahydrofuran	Under vacuum	
Py-CoSi–PMMA	Chloroform	Under atmosphere	Yes

blue-shifted exciplex emission and its intensity is a little smaller, compared with (a), which was dried sufficiently.

Fluorescence spectra of samples (c) and (d) are shown in Fig. 2. There were some differences between the spectra in respect with intensity ratios of exciplex emission to monomer emission (I_e/I_m) and λ_{max} of exciplex. Sample (c) displayed significant blue-shift emission maximum and sample (d) showed red-shift and larger I_e/I_m compared with sample (a). Such sensitivity of exciplex emission to the preparative conditions of the samples reflected the existence of more than two species in different microenvironments.

For more information on these exciplex species, fluorescence decay curves were measured. The monitoring wavelength was 398 nm to follow monomer fluorescence, whereas wavelengths at 480 and 540 nm were selected

for tracing exciplex emission at a shorter and a longer wavelength of the exciplex. The decay curves were deconvoluted into multiple exponential elements and were well analyzed as triple exponential decay components and no rise components. A typical fitting curve is shown in Fig. 3 and its $\chi^2 = 1.13$. χ^2 values for all samples were 1.08–1.19 and the residuals were also small and well-balanced in the plus side and the minus side, which were good enough to trust the data.

Fluorescence lifetimes at various wavelengths are summarized in Table II. The fact that there was no rise lifetime indicated that exciplex did not form dynamically with movement of the polymer segment when pyrenyl units were excited. It also revealed that there were performed ground-state complexes of pyrenyl group and DMA, and exciplex forms just after pyrenyl groups adsorbed excited
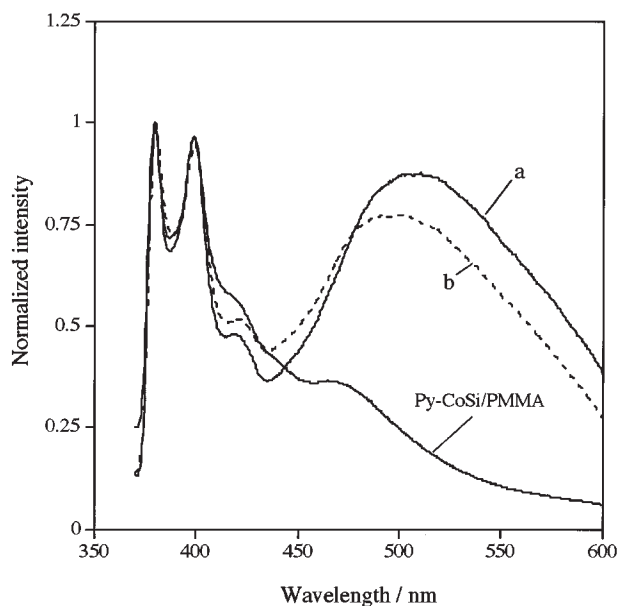

Fig. 1. Fluorescence spectra of Py-CoSi–**2** prepared with chloroform solutions [sample (a): solid line; sample (b): dotted line] see Table I) and Py-CoSi–PMMA normalized at λ_{max} of monomer emission.
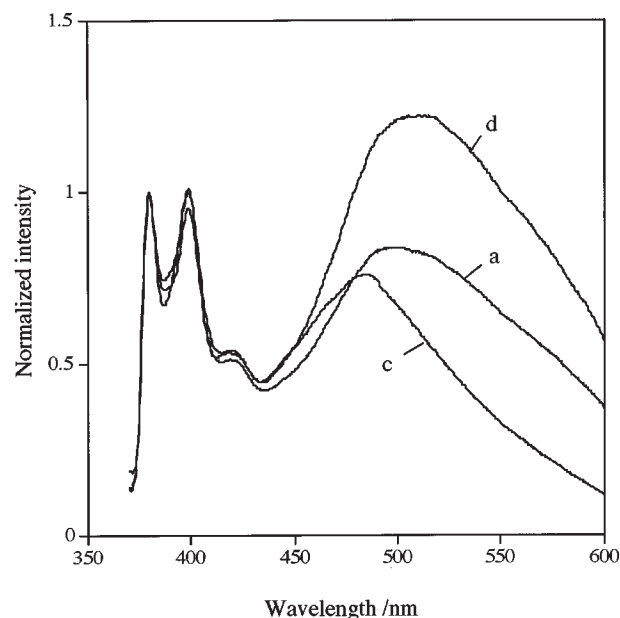
Fig. 2. Fluorescence spectra of Py-CoSi–**2** prepared with chloroform solution [sample (a) see (Table I)] and tetrahydrofuran solutions [samples (c) and (d) see (Table I)] normalized at λ_{max} of monomer emission.
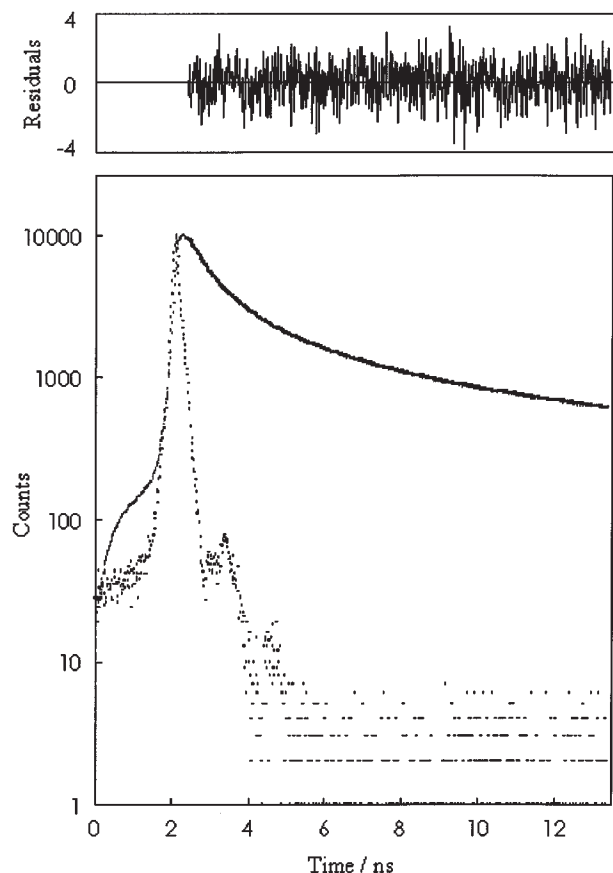
Fig. 3. Time-resolved profile for Py-CoSi–**2** sample (a), the excitation light profile and the fitting curve (see Table II) (below) and residuals of fitting curve (above).

light without movement of the polymer segments. There was no distinct difference in the lifetimes between the samples prepared under various preparative conditions.

The triple exponential fitting was just an expedient and it did cause us to conclude that there were three kinetic decay paths in these systems. However, some lifetimes indicated interesting results. The lifetime constants of Py-CoSi–PMMA at 398 and 480 nm were not far from each other because they all came from monomer emission. In contrast, for the samples covered with **2**, the longest lifetime (τ_3) of exciplex emission was longer than that of monomer emission, whereas the shortest and the middle lifetimes (τ_1, τ_2) were almost the same. τ_3 of monomer emission of the samples with **2** was close to that of Py-CoSi–PMMA. The intensity ratios of τ_3 of exciplex emission were larger at 540 nm than at 480 nm. It could be assumed from these data that 11 and 16 ns for τ_3 were lifetimes of monomer and exciplex formed from ground-state complex, respectively. On the other hand, the other kinetic paths, to which τ_1 and τ_2 were related, showed deactivation by energy transfer to polymer matrix or colloidal silica surface. On the basis of these, it was assumed that pyrenyl groups on silica surface and DMA units attached to polymer backbones form ground-state complexes at the polymer–silica interface, leading to the diversified distribution of energy states, whereas their exciplex states have similar lifetimes. According to these results, it can be considered that τ_1 and τ_2 did not indicate the deactivation lifetime, but indicated the representative values of numerous deactivation paths. Exciplex originated from a ground-state complex with a lower energy emitted at a shorter wavelength because it deactivated to the same ground-state complex as a result of a fixed matrix.

The distributions of ground state complexes, which gave the various exciplex emission intensity and wavelength, depended on preparative conditions. There are

Table II. Fluorescence Lifetimes

λ_{mon}	398 nm			480 nm			540 nm		
	τ_1/ns[b] Amp$_1$[a]	τ_2/ns Amp$_2$	τ_3/ns Amp$_3$	τ_1/ns Amp$_1$	τ_2/ns Amp$_2$	τ_3/ns Amp$_3$	τ_1/ns Amp$_1$	τ_2/ns Amp$_2$	τ_3/ns Amp$_3$
Py-CoSi–**2** (a)	0.53	2.0	9.7	0.53	2.2	15.2	0.56	3.1	16.7
	0.32	0.44	0.24	0.68	0.23	0.08	0.61	0.22	0.17
Py-CoSi–**2** (b)	0.51	2.6	12.3	0.56	2.2	14.7			
	0.70	0.25	0.06	0.66	0.26	0.08			
Py-CoSi–**2** (c)	0.62	2.8	11.9	0.50	2.0	15.6	0.63	2.4	17.0
	0.45	0.37	0.18	0.51	0.39	0.10	0.54	0.33	0.14
Py-CoSi–**2** (d)	0.57	2.5	10.9	0.49	2.3	15.6	0.41	2.3	15.2
	0.32	0.47	0.21	0.59	0.28	0.13	0.49	0.30	0.21
Py-CoSi–PMMA	0.81	2.6	12.6	0.68	1.9	12.7			
	0.44	0.39	0.17	0.72	0.22	0.07			

[a] Amp: relative values (Amp$_1$ + Amp$_2$ + Amp$_3$ = 1).
[b] Errors: of τ's are: τ_1 ± 0.06 ns, τ_2 ± 0.2 ns, τ_3 ± 1.9 ns.

several possibilities to explain the different exciplex emission between the samples. The most considerable one between samples (a) and (b) is as follows: residual chloroform molecules solvated the ground-state complex to make their energy level lower to emit at a little shorter wavelength for sample (b). One of the possibilities of the remarkable blue-shift of exciplex emission of sample (c) prepared from a THF solution compared with sample (a) prepared from a chloroform solution, can be explained as follows. Polymer chains of **2** expanded by the solvation in a THF solution to form a more stable ground-state complex with pyrenyl groups on silica than for a chloroform solution, because THF solvates methacrylate polymer better than does chloroform. Slow evaporation froze the stable complex, which had been made in a solution, at the polymer–silica interface, and showed exciplex emission at shorter wavelength compared to that prepared from a chloroform solution. Sample (d), which was prepared from a THF solution and was subjected to fast solvent evaporation, showed stronger exciplex emission at a longer wavelength region compared with others that were prepared by slow evaporation. In this case, the evaporating process was too fast to solvate the side-chain DMA during evaporation, and it kept DMA units faced at the interface to produce many unstable ground-state complexes, which showed red-shift exciplex emission. Fewer side-chain DMA units could get into the polymer bulk during fast evaporation.

Annealing Effects

The samples prepared under various conditions were annealed to check the alteration of fluorescence behavior. Figure 4 shows fluorescence spectra of sample (a) during annealing. The intensity of broad emission at the longer wavelength region increased and the λ_{max} moved slightly to shorter wavelength during annealing at 105°C, which is 2°C below T_g of **2**, for 30 min. However, annealing at 105°C for more than 30 min did not cause any more change. These phenomena were the same for sample (b), in which some solvent remained at first. For comparison, a sample that **2** coated on nontreated colloidal silica and Py-CoSi–PMMA was also annealed at 105°C. The PMMA sample did not display any change in fluorescence behavior during annealing, implying that the increase in emission intensity at longer wavelengths of Py-CoSi covered with **2** was not caused by interactions between pyrenyl groups themselves. On the other hand, it was also confirmed that the emission at the longer wavelength region during annealing was not due to DMA units, be-
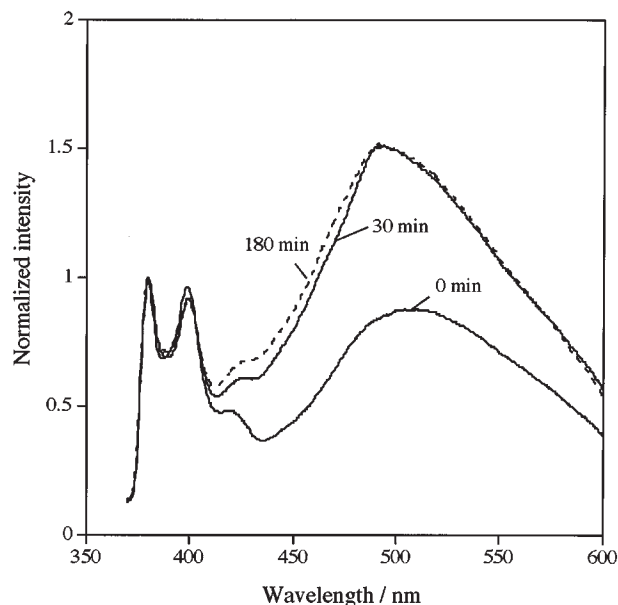

Fig. 4. Fluorescence spectra of Py-CoSi–**2** sample (a) annealed at 105°C for 0, 30 (solid line), and 180 min (broken line) normalized at λ_{max} of monomer emission.

cause nontreated colloidal silica coated by **2** showed no spectral change during annealing. These data also support the belief that the broad emission at longer wavelengths is assigned to exciplex.

Fluorescence lifetimes were not altered before and after the annealing, as shown in Table III. This result suggested that the microenvironment of pyrene–DMA ground-state complex at Py-CoSi–**2** interface did not change drastically, although the complex population increased during annealing at temperatures just below T_g.

When the annealing temperature was 90°C, the spectral changes were almost same as those at 105°C. However, the changing process took longer time than for the 105°C annealing. I_e/I_m increased at the initial period in 30 min and the population of exciplex that emits at shorter wavelength region increased after 30 min annealing.

In comparison with the annealing at the temperature below T_g, the annealing effect at 120°C, which was higher than T_g by 13°C, was different. The increment of the I_e/I_m was not saturated at 30 min and the spectrum moved to a shorter wavelength than for the case of 105° or 90°C. The lifetimes were also changed dynamically after 210 min of annealing. τ_3 became shorter and shorter during annealing; the result was that the fluorescence decay curves could not be fitted with triple-exponential any more and were analyzed as double-exponential time constants. The longest time constant, which was assigned to exciplex lifetime, and middle time constants became close and combined as τ_2. It can be considered that the annealing at the

Table III. Fluorescence Lifetimes of Annealed Samples

	λ_{mon}		480 nm			540 nm		
	Annealing		τ_1/ns^c	τ_2/ns	τ_3/ns	τ_1/ns	τ_2/ns	τ_3/ns
	Temperature °C	Time (min)	$Amp_1{}^a$	Amp_2	Amp_3	Amp_1	Amp_2	Amp_3
Py-CoSi–**2** (a)	105	180	0.61	2.3	17.8			
			0.62	0.28	0.09			
Py-CoSi–**2** (a)	120	30	0.46	1.9	12.6			
			0.49	0.39	0.12			
Py-CoSi–**2** (a)	120	210	0.73		6.6^b	0.94		10.9^b
			0.84		0.16	0.74		0.26
Py-CoSi–**2** (c)	105	180	0.57	2.2	16.1	0.49	2.2	16.6
			0.57	0.31	0.12	0.42	0.33	0.25

[a] Amp: relative values ($Amp_1 + Amp_2 + Amp_3 = 1$).
[b] Double exponential.
[c] Errors: of τ's are: $\tau_1 \pm 0.06$ ns, $\tau_2 \pm 0.2$ ns, $\tau_3 \pm 1.9$ ns.

temperature higher than T_g for a long time produced the polymer chain movement to the interfacial layer that was more intricate than annealing below T_g to make the population of performed ground-state sites large, and their microenvironments were ordered to be easily deactivated.

The spectra of the samples from THF solution after annealing at 105°C are shown in Figs. 5 and 6. Although the annealing of sample (c) prepared by slow evaporation enhanced the spectral intensity, the spectral shape was almost maintained during annealing. There was no

remarkable change in fluorescence lifetimes of sample (c), as shown in Table III. These results suggest that the microenvironment of preformed ground-state complexes produced just after evaporation was at the most stable energy level and the population of DMA units that faces to the silica surface increased during annealing. The spectrum of sample (d) prepared by fast evaporation under vacuum moved to a shorter wavelength region, although I_e/I_m was almost same. These results can be interpreted that the fast evaporation froze the orientation of DMA
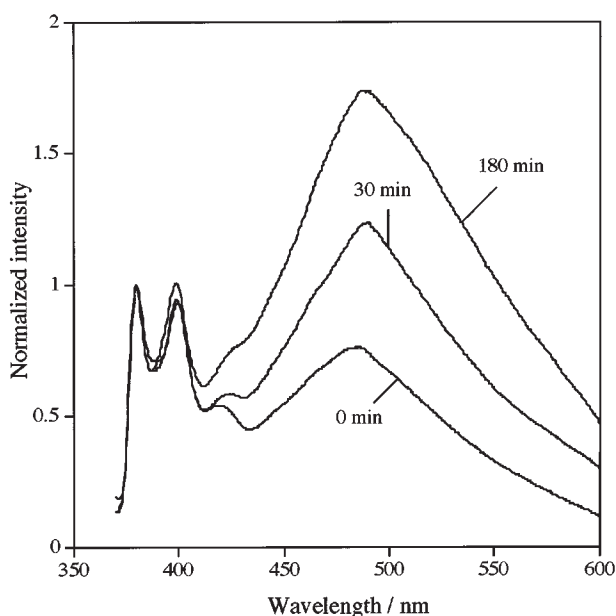

Fig. 5. Fluorescence spectra of Py-CoSi–**2** sample (c) annealed at 105°C for 0, 30, and 180 min normalized at λ_{max} of monomer emission.
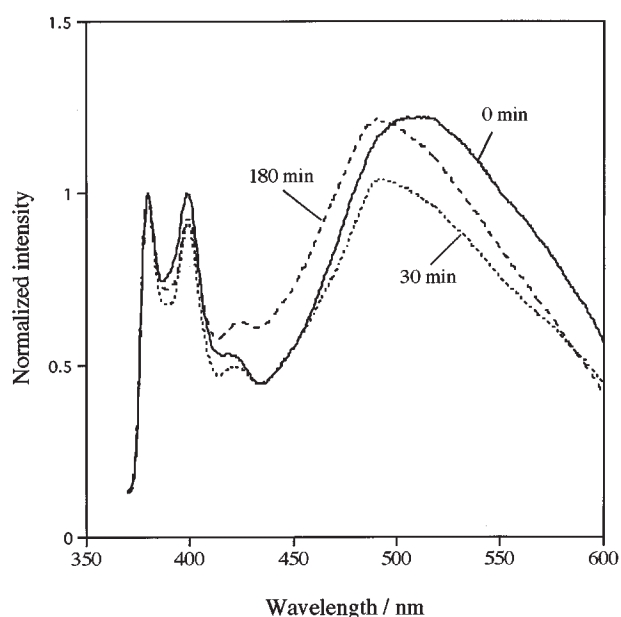

Fig. 6. Fluorescence spectra of Py-CoSi–**2** sample (d) annealed at 105°C for 0 (solid line), 30 (dotted line), and 180 min (broken line) normalized at λ_{max} of monomer emission.

units that faced to the silica surface to make performed exciplex sites, which maintained the I_e/I_m value, and their microenvironment changed to the stable energy state during annealing because the first frozen conformation of performed site was unstable. The result that the spectrum of the sample annealed for 180 min was similar to the spectra of the other samples annealed under T_g for 180 min supports the above interpretation.

The Most Stable Microenvironment at Polymer–Silica Interface

As described above, the fluorescence spectra of all Py-CoSi–**2** prepared from chloroform and THF became similar to each other after annealing. Furthermore, emission spectra of the samples that had been stored at room temperature for 1 month were also measured. The spectra became the same as each other and the same as the spectrum of sample (a) annealed for 180 min shown in Fig. 4, which was same as that of annealed sample (b) at the temperature below T_g. λ_{max} was 490 nm and I_e/I_m was 1.6. The samples prepared from THF that had been kept at room temperature for 1 month also gave the same spectra. The exciplex spectrum shifted to the longer wavelength region and I_e/I_m slightly decreased for sample (c), whereas the exciplex spectral shape did not change from the sample annealed for 180 min, although I_e/I_m increased for sample (d). Even sample (a) annealed at 120°C showed the same emission after 1 month although its I_e/I_m had been larger than 2. This spectrum can be assigned as the final state of the movement of the polymer segments possessing DMA to the most stable position. The first state of the microenvironment of solid–polymer interface depends on the preparation conditions, but annealing made the interfacial microenvironment the same and at most stable state, which does not depend on the initial conditions. It was also revealed that the annealing below polymer T_g in a few hours makes the microenvironment of silica–polymer interface orientate to the most stable form. Though the annealing above T_g makes the interface layer microenvironment intricate, the polymer segments move to the most stable form when they are maintained at room temperature for a long time, such as 1 month.

CONCLUSIONS

Molecular interaction between a functional group modified on silica surface and another functional group of polymer that was coated on the silica was observed with static and dynamic fluorescence measurements. Pyrene and DMA were adopted for the functional groups

modified on silica and polymer, respectively. Pyrene was linked to silica surface through a CRA framework to maintain the distance between pyrenyl groups and avoid making excimer. DMA was imported in methacrylate polymer as a side-chain substitute. The molecular interaction at the interface of two materials was observed as exciplex emission.

It was considered that there were several types of sites of the functional groups at the interface, such as independent pyrene monomer sites, pyrene–DMA preformed exciplex sites, and the sites where exciplex could be formed by movement of polymer segment DMA to pyrene. It was revealed that the population of each site depended on the sample preparation conditions, such as used solvents of the polymer and the speed at which the solvent evaporated.

The annealing effects were also observed. λ_{max} of exciplex moved to shorter wavelength and I_e/I_m increased. However, the ways in which the emission spectra changed also depended on the initial conditions and the annealing temperature. Exciplex wavelength indicates the difference between the energy of the excited state and the ground state, and I_e/I_m reflects the population of each site. During annealing, the distribution of exciplex population and the microenvironment of the exciplex site became the same and formed the most stable state, although the initial distribution and microenvironment depended on the sample preparation conditions.

REFERENCES

1. Y. Hayashi, Y. Kawada, and K. Ichimura (1995) Dicyanoanthracene as a fluorescence probe for studies on silica surfaces. *Langmuir* **11**(6), 2077–2082.
2. A. Takahara, T. Magome, and T. Kajiyama (1994) Effect of glass fiber-matrix polymer interaction on fatigue characteristics of short glass fiber reinforced Poly(butylene terephthalate) based on dynamic viscoelastic measurement during the fatigue process. *J. Polym. Sci. B* **32**(5), 839–849.
3. M. Afeworki, R. A. Mckay, and J. Schaefer (1993) Dynamic nuclear polarization enhanced nuclear magnetic resonance of polymer-blend interfaces. *Mater. Sci. Eng. A* **162**(1–2), 221–228.
4. R. Lazzaroni, C. Gregoire, M Chtaib, and J. J. Pireaux (1992) The metal/polyaniline interface: an X-ray photoelectron spectroscopy study. *Polymer-Solid Interfaces Proc. 1st Int. Conf.* 213–214.
5. (a) K. Hara, P. de Mayo, W. R. Ware, W. A. C. Weeden, G. S. K. Wong, and K. C. Wu (1980) Biphasic Photochemistry: Time-resolved spectra of adsorbed hydrocarbons. *Chem. Phys. Lett.* **69**(1), 105–108. (b) R. K. Bauer, P. de Mayo, W. R. Ware, and K. C. Wu (1982) Surface photochemistry: The photophysics of pyrene adsorbed on silica gel, alumina and calcium fluoride. *J. Phys. Chem.* **86**(19), 3781–3789. (c) R. K. Bauer, P. de Mayo, L. V. Natarajan, and W. R. Ware (1984) Surface photochemistry: The effect of surface modification on the photophysics of naphtalene and pyrene adsorbed on silica gel. *Can. J. Chem.* **62**(7), 1279–1286. (d) P. de Mayo, L. V. Natarajan, and W. R. Ware (1985) Surface photochemistry Temperature effects on the emis-

sion of aromatic hydrocarbons adsorbed on silica gel. *ACS Symp. Ser.* **278**, 1–19.

6. (a) C. H. Lochmüller, A. S. Colborn, M. L. Hunnicutt, and J. M. Harris (1983) Organization and distribution of molecules chemically mound to silica. *Anal. Chem.* **55**(8), 1344–1348. (b) C. H. Lochmüller, A. S. Colborn, M. L. Hunnicutt, and J. M. Harris (1984) Bound pyrene excimer photophysics and the organization and distribution of reaction sites on silica. *J. Am. Chem. Soc.* **106**(15), 4077–4082. (c) C. H. Lochmüller and M. J. Hunnicutt (1986) Solvent-induced conformational changes on chemically modified silica surfaces. *J. Phys. Chem.* **90**(18), 4318–4322. (d) C. H. Lochmüller and M. T. Kersey (1988) Effect of thermal pretreatment on the surface reactivity of amorphous silica. *Langmuir* **4**(3), 572–578.

7. (a) P. Hite, R. Kransansky, and J. K. Thomas (1986) Spectroscopic investigations of surfaces using aminopyrene. *J. Phys. Chem.* **90**(22), 5795–5799. (b) M. A. T. Marro and J. K. Thomas (1993) Movement of small molecules on silica surface: photophysical and photochemical study. *J. Photochem. Photobiol.* **A72**(3), 251–259.

8. P. Somasundaran, S. Krishnakumar, and J. T. Kunjappu (1995) Spectroscopic characterization of surfactant and polymer solloids (surface colloids) at solid-liquid interface. *ACS Symp. Ser.* **615**, 104–137.

9. S. H. Chen and C. W. Frank (1995) Fluorescence probe studies of self-assembled monolayer and multilayer films from n-alkyltrichlorosilanes. *ACS Symp. Ser.* **615**, 217–230.

10. J. B. Birks (1969) *Photophysics of Aromatic Molecules,* Wiley-Interscience, London, p. 403.

11. N. Mataga, T. Okada, and N. Yamamoto (1966) The luminescence of the heteropolar excimer in the cyclohexane matrix. *Bull. Chem. Soc. Jpn.* **39**(11), 2562–2562.

12. N. Mataga, T. Okada, and N. Yamamoto (1967) Electronic processes in hetro excimers and mechanism of fluorescence quenching. *Chem. Phys. Lett.* **1**(4), 119–121.

13. K. Ichimura, N. Fukushima, M. Fujimaki, S. Kawahara, Y. Matsuzawa, Y. Hayashi, and K. Kudo (1997) Macrocyclic Amphiphiles Properties of calix[4]resorcinarene derivatives subtituted with azobenzenes in solutions and monolayers. *Langmuir* **13**(25), 6780–6786.

14. K. Ichimura, M. Fujimaki, Y. Matsuzawa, Y. Hayashi, and M. Nakagawa (1999) Characteristics of monolayers of calix[4]resorcinarenes derivatives having azobenzene chromophores. *Mat. Sci. Eng. C* **8–9**, 353–359.

15. E. Kurita, N. Fukushima, M. Fujimaki, Y. Matsuzawa, K. Kudo, and K. Ichimura (1998) Macrocyclic amphiphiles. Part 2. Multi point adsorptivity of the crown conformer of calix[4]resorcinarenes and their derivatives on surfaces of amorphous polar substrates. *J. Mater. Chem.* **8**(2), 397–404.

16. Y. Hayashi, T. Maruyama, T. Yachi, K. Kudo, and K. Ichimura (1998) Synthesis and fluorescence behavior of calix[4]resorcinarenes possessing pyrenyl group(s). *J. Chem. Soc. Perkin Trans. 2* **4**, 981–997.

17. S. E. Klassen, G. H. Daub, and D. L. VanderJagt (1983) Carbon 13 labeled benzo[a]pyrenes and derivatives, 4. Labeling the 7–10 positions. *J. Org. Chem.* **48**(23), 4361–4366.